Journal of Applied Polymer Science

# Electrospun poly(hydroxybutyrate)/chitosan blend fibrous scaffolds for cartilage tissue engineering

**Davoud Sadeghi,[1,2] Saeed Karbasi,[1] Shahnaz Razavi,[3] Sajjad Mohammadi,[2] Mohammad Ali Shokrgozar,[2] Shahin Bonakdar[2]**

[1]Department of Biomaterials and Tissue Engineering, School of Advance Technology in Medicine, Isfahan University of Medical Sciences, Isfahan, Iran

[2]National Cell Bank, Pasteur Institute of Iran, Tehran, Iran

[3]Department of Anatomical Sciences, School of Medicine, Isfahan University of Medical Sciences, Isfahan, Iran

Correspondence to: S. Karbasi (E-mail: Karbasi@med.mui.ac.ir) and S. Bonakdar (E-mail: Sh_bonakdar@pasteur.ac.ir)

**ABSTRACT:** In this study, polyhydroxybutyrate (PHB) was blended with chitosan (CTS), and electrospun in order to produce more hydrophilic fibrous scaffolds with higher mass loss rates for cartilage tissue engineering application. First, the effects of diverse factors on the average and distribution of fiber's diameter of PHB scaffolds were systematically evaluated by experimental design. Then, PHB 9 wt % solutions were blended with various ratios of CTS (5%, 10%, 15%, and 20%) using trifluoroacetic acid as a co-solvent, and electrospun. The addition of CTS could decrease both water droplet contact angle from ~74° to ~67° and tensile strength from, ~87 MPa to ~31 MPa. According to the results, the scaffolds containing 15% and 20% CTS were selected as optimized scaffolds for further investigations. Mass loss percentage of these scaffolds was directly proportional to the amount of CTS. Chondrocytes attached well to the surfaces of these scaffolds. The findings suggested that PHB/CTS blend fibrous scaffolds have tremendous potentials for further investigations for the intended application. © 2016 Wiley Periodicals, Inc. J. Appl. Polym. Sci. **2016**, *133*, 44171.

**KEYWORDS:** biomaterials; blends; electrospinning; hydrophilic polymers; properties and characterization

Received 25 December 2015; accepted 8 July 2016

**DOI: 10.1002/app.44171**

## INTRODUCTION

Adult articular cartilage tissue exhibits a limited inherent capacity for regeneration and repair so that cartilage tissue defects often lead to osteoarthritis, ultimately necessitating total joint replacement.[1,2] Nowadays, many surgical techniques, including autografts, allografts, and xenografts, are employed to treat cartilage tissue defects. Despite success reports, these methods have some drawbacks which limit their widespread application. Cartilage tissue engineering is a novel approach that uses a combination of cells, scaffold, and growth factors to regenerate lost or damaged cartilage tissue to overcome restrictions of the conventional clinical methods.[3–6] An ideal scaffold should mimic native extracellular matrix (ECM) of the target tissue to support cell activities and new tissue formation processes.[7,8] Electrospinning process has shown considerable potential to produce fibrous scaffolds that can mimic natural tissue's ECM structure.[9] Electrospun fibrous scaffolds exhibit many good structural properties, including high surface area, higher porosity, and interconnected pores, which promote cell stimulation and nutrient/waste product exchange.[10,11] To date, many natural and synthetic polymers have been explored for fabrication of fibrous scaffolds via the electrospinning process.[12,13] Polyhydroxybutyrate (PHB) is a natural polymer with promising properties such as good biocompatibility and high mechanical strength in comparison with other natural polymers. However, PHB suffers from its low hydrophilicity and very slow mass loss rate, especially in case of cartilage tissue engineering application.[14–18] Blending with other polymers is an approach to overcome the restrictions of PHB. To date, many synthetic polymers, including poly(hydroxybutyrate-hydroxyhexanoate) (PHBHHx), poly (hydroxybutyrate-valerate) (PHBV), polyaniline (PA), poly(ε-caprolactone), and so forth, have been blended with PHB.[19–22] However, blending these polymers with PHB has overcome only one of the limitations of PHB specifically. Chitosan (CTS) is a natural polymer which, besides its advantages such as biocompatibility, nontoxicity, antibacterial activity, high availability and low cost, benefits from its relatively high mass loss rate and hydrophilicity.[23] In addition, it has been reported that CTS can support chondrogenic activities and facilitate articular cartilage repair.[24–27] Therefore, such properties of PHB including mass loss rate, hydrophilicity, and biological properties can be promoted through blending with CTS.

**Table I.** Designed Experiments by *MiniTab 16* Software Using Taguchi Algorithm

| Experiment code | PHB concentration (wt %) | Distance (cm) | Voltage (kVp) |
|---|---|---|---|
| P1 | 7 | 7 | 9 |
| P2 | 7 | 14 | 13 |
| P3 | 8 | 7 | 9 |
| P4 | 8 | 14 | 13 |
| P5 | 9 | 7 | 13 |
| P6 | 9 | 14 | 9 |
| P7 | 10 | 7 | 13 |
| P8 | 10 | 14 | 9 |

In this study, PHB/CTS blend solution was electrospun and optimized for cartilage tissue engineering application. Trifluoroacetic acid (TFA) was used as co-solvent of PHB and CTS.[28] The fabricated scaffolds were then characterized by scanning electron microscopy (SEM), Fourier transform infrared spectroscopy (FTIR), water contact angle measurement, tensile strength test, *in vitro* mass loss assay and cell attachment study. Results showed that electrospinning of PHB/CTS blend solutions could produce more hydrophilic fibrous scaffolds with higher mass loss rate compared to the electrospun PHB fibrous scaffolds, which is more favorable for cartilage tissue engineering application.

## EXPERIMENTAL

### Materials

PHB powder ($M_w = 300{,}000$; CAS number = 3-00-26063), CTS (medium molecular weight, dd = 75–85%), trypsin, L-glutamine and glutaraldehyde (GTA) were purchased from Sigma-Aldrich (St. Louis, Missouri, United States). TFA (purity > 99%, 1.49 g $mL^{-1}$) was purchased from Carlo Erba (Rodano, Italy). Dulbecco modified Eagle medium (DMEM) and penicillin–streptomycin were purchased from Gibco-BRL, Life Technologies (Rockville, Maryland, United States). Fetal bovine serum (FBS) was purchased from NanoBioArray (Tehran, Iran). The Software *MiniTab 16* was employed for designing of experiments. Images were analyzed by the *Image J* software (National Institute of Health (NIH), USA). The Software *CorelDraw X5* was used to design and draw the graphical abstract. All plots were drawn by the software *OriginPro 9.1*.

### Design of Experiment

Taguchi method provides an opportunity to identify effects of each factor on the obtained results.[29,30] This method has three main steps: (1) selecting factors, defining the levels of each factor and planning the experiments, (2) executing the designed experiments, and (3) evaluating the results. The number of factors that needed to be evaluated as well as their levels are determined in the first step.[31,32] In this study, based on the authors' experiences and literature review, three factors, i.e., polymer solution concentration, applied voltage (V) and tip-to-collector distance (D) were selected as more effective factors on the electrospinning process of PHB polymeric solution. Four levels of concentration and two levels of the both V and D were determined. For the design of experiments based on the chosen factors and related levels, a standard L-8 OA was employed and then the designed experiments were executed (Table I). Finally, the impacts of each factor on two considered response variables, including average and distribution (coefficient of variation; C.V.) of fiber's diameter of the scaffolds, were statistically analyzed by *MiniTab 16* software. The C.V. of the fiber's diameter was calculated as a criterion of the distribution of fiber's diameter using eq. (1):

$$\text{C.V.} = \frac{\sigma}{\mu} \quad (1)$$

Where, σ and μ are standard deviation (SD) and mean of fiber's diameter, respectively.

### Electrospinning of PHB/CTS Blend

Based on the designed experiments, diverse concentrations of PHB polymeric solutions were prepared through the dissolving PHB in TFA by magnetic stirring for 4 h at 25 ± 2 °C, and electrospun under various Vs and Ds. Since uniformity of the fibers had been considered as a more important feature than fiber diameter, and according to the results of the statistical analyses, further optimization of electrospinning conditions of selected specimen from the first step (P5) was performed with the aim to obtain more uniform fibers. For this aim, PHB polymeric solution (9 wt %) was electrospun under various Vs and Ds (Table II). In the next step, V and D of the optimized specimen (V = 21 kVp, D = 15 cm) were applied to electrospun PHB (9 wt %)/CTS blend solutions, which were prepared by dissolving various percentages of CTS (5%, 10%, 15%, and 20%) in PHB solution by magnetic stirring for 2 h at 25 ± 2 °C. At all the steps, syringes with a 21G needle were used and the flow rate was adjusted at 0.5 mL $h^{-1}$ for electrospinning of polymeric solutions.

### SEM Imaging

The surface morphology of the electrospun fibrous scaffolds was observed by SEM (TESCAN, VegaII, Czech). Surfaces of the fibrous scaffolds were sputter-coated with gold (Au) prior to the examination. The diameter of the fibers was calculated from the SEM images by *Image J* software.

**Table II.** Various applied Vs and Ds on Electrospinning of PHB 9 wt % Solution

| Sample | PHB concentration (wt %) | Distance (cm) | Voltage (kVp) |
|---|---|---|---|
| S1 | 9 | 11 | 9 |
| S2 | 9 | 7 | 13 |
| S3 | 9 | 15 | 13 |
| S4 | 9 | 11 | 17 |
| S5 | 9 | 15 | 17 |
| S6 | 9 | 7 | 21 |
| S7 | 9 | 11 | 21 |
| S8 | 9 | 15 | 21 |

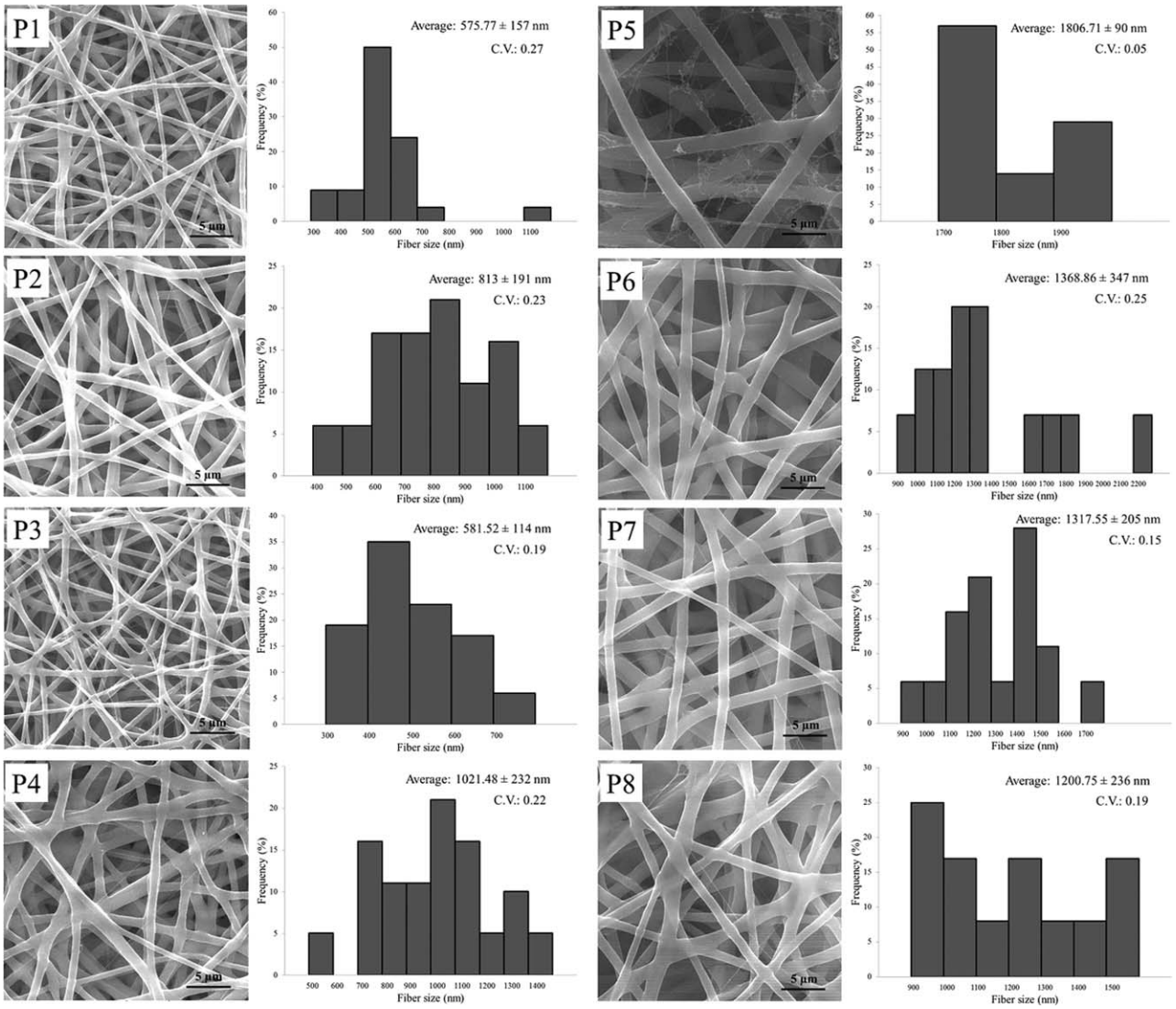


**Figure 1.** SEM images of the pure PHB fibrous scaffolds: (P1) 7 wt %, D = 7 cm, V = 9kVp, (P2) 7 wt %, D = 14 cm, V = 13kVp, (P3) 8 wt %, D = 7 cm, V = 9kVp, (P4) 8 wt %, D = 14 cm, V = 13kVp, (P5) 9 wt %, D = 7 cm, V = 13kVp, (P6) 9 wt %, D = 14 cm, V = 9kVp, (P7) 10 wt %, D = 7 cm, V = 13kVp, (P8) 10 wt %, D = 14 cm, V = 9kVp.

### FT-IR Analysis

To investigate chemical interactions between the PHB and CTS, FT-IR analysis was performed using a Tensor 27 FTIR apparatus (Thermo Nicolet) between 400 and 4000 $cm^{-1}$. The scaffolds were scratched into powder, mixed with KBr powder, and then compressed into pellets, prior to investigation.

### Porosity

The porosity of the scaffolds was determined using a method described by Chakrapani *et al.*[33] Briefly, the scaffolds were cut into rectangular strips of 10 × 20 mm dimensions and weighed. The thickness of the strips was measured using an SDL 94 thickness gauge (Shirley Developments Ltd., Stockport, England). Density and porosity of the scaffolds were determined using eqs. (2) and (3):

$$\text{Density} = \left(\frac{\text{mass of scaffold}}{\text{area of scaffold} \times \text{thickness of scaffold}}\right) \quad (2)$$

$$\text{Porosity } (\%) = \left(1 - \frac{\text{scaffold density}}{\text{bulk material density}}\right) \times 100 \quad (3)$$

The bulk density of PHB and CTS were considered 1.24 gm $L^{-1}$ and 0.3 gm $L^{-1}$, respectively.[34,35]

### Water Contact Angle

Thin Films of PHB and PHB/CTS blend solutions were prepared by casting into Petri dishes and drying in an oven (30 ± 4 °C) and water contact angle (WCA) of the samples was measured by sessile drop method using a G10 contact angle goniometer (Kruss, Germany) at 25 ± 2 °C. Distilled water droplet was mounted on the surface of each sample and the contact angle was measured after 10 s. Measurements were performed at five independent points of each sample and expressed as mean ± SD.

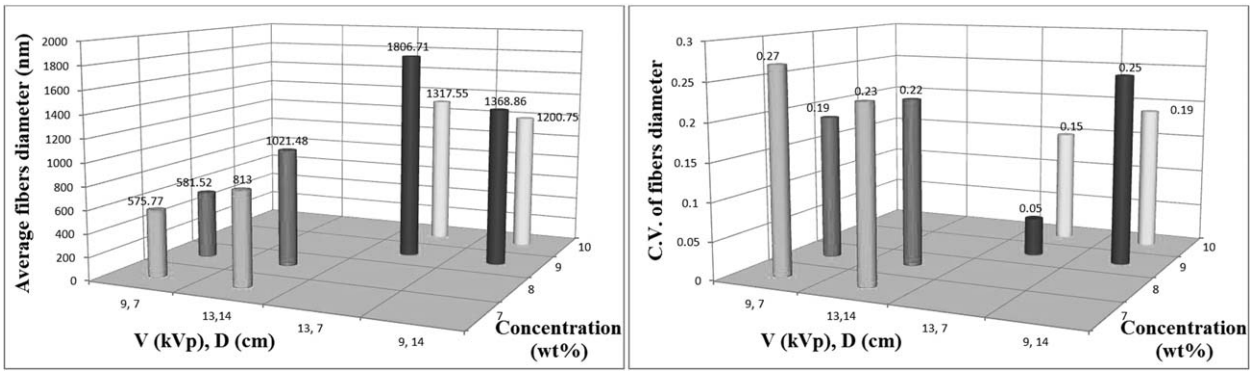


**Figure 2.** The effects of various factors on average (left) and C.V. (right) of fiber's diameter.

### Tensile Strength

The tensile test of nanofibrous scaffolds was performed according to ASTM D882-12 (2012)[36] using a uniaxial tensile machine (INSTRON 5566, USA) and a load cell of 50 *N* capacity. The scaffolds were cut into rectangular strips of 1 × 2 cm dimensions and fixed vertically on the gripping unit of the tensile tester. Moreover, the specimens were drawn at a crosshead speed of 20 mm $min^{-1}$ and data were recorded every 50 ms.

### Mass Loss

The electrospun scaffolds were cut into square shapes, weighed and placed in well plates. The wells were filled with phosphate-buffered saline (PBS; pH∼7.4) and incubated at 37 ± 2 °C with the aim to mimic natural biological environment. The PBS buffer was changed every 3–4 days and the degraded specimens were extracted every week over a 2-month period. At the time of extraction, the specimens (3 replicates) were taken out from the incubator, washed with distilled water and vacuum-dried at 40 °C for 48 h to constant weight. The specimens were weighed at specified intervals to calculate the mass loss using eq. (4).

$$\text{Mass loss } (\%) = \left(\frac{\text{Mo} - \text{Mt}}{\text{Mo}}\right) \times 100 \qquad (4)$$

Where $M_o$ and $M_t$ are the dry masses of the specimens before and after the mass loss, respectively.

### Cell Attachment

Chondrocyte cells isolated from rabbit's articular cartilage tissue were freshly provided by National Cell Bank of Iran, Pasteur Institute of Iran, Tehran, Iran. The medium consisted of Dulbecco modified Eagle medium-Hams F12 supplemented with 10% FBS and 100 μg $mL^{-1}$ of penicillin–streptomycin was used.

To investigate cell attachment to the surfaces of the electrospun scaffolds, 5 × $10^5$ chondrocytes were seeded on each specimen and incubated for 4 h. After removal of the culture medium, the specimens were rinsed with PBS twice and the cells were then fixed with 4% GTA solution. In order to observe chondrocyte's attachment and morphology on the scaffolds by SEM, the fixed cells were dehydrated in graded alcohol solutions and sputter-coated with gold.

### Statistical Analysis

All the experiments were carried out at least three times and the average of the results was expressed as mean ± SD. Statistical calculations were performed for all the data at a statistical significance level of $P < 0.05$.

## RESULTS AND DISCUSSION

### SEM Investigations

Morphology of the electrospun fibrous scaffolds is affected by diverse parameters such as applied V, D, the flow rate of the solution, polymer concentration and solution viscosity.[37]

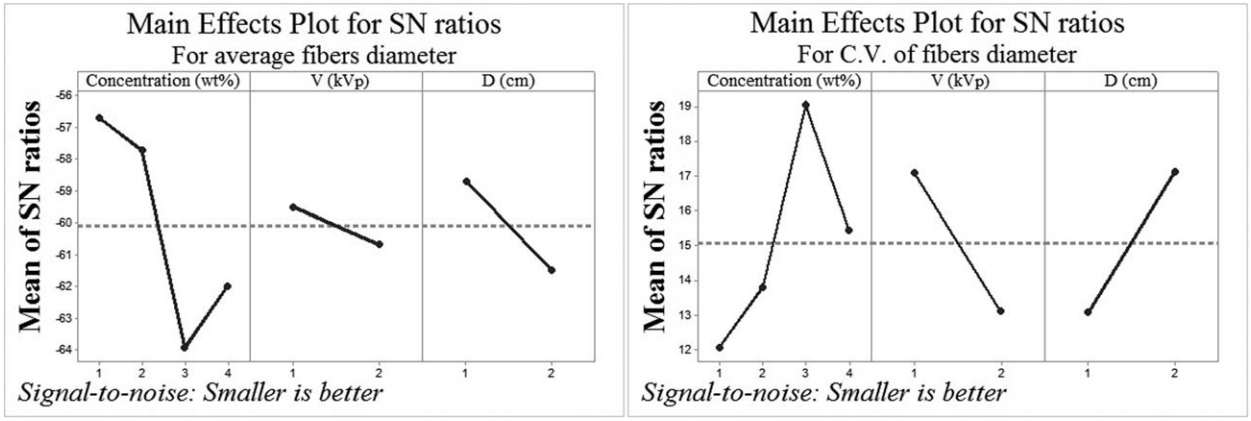


**Figure 3.** S/N ratios plots for average (left) and C.V. (right) of fiber's diameter.

Both the SEM images and distribution of fiber's diameter of the fibrous scaffolds produced based on Table I are shown in Figure 1. As it can be observed, all the fibrous scaffolds lacked beads. The specimen P1 has the minimum average fiber diameter (575.77 nm) and maximum C.V. (0.27), while the specimen P5 has the maximum average fiber size (1806.71 nm) and minimum C.V. (0.05). In each concentration, there is a direct relationship between average fiber size and applied voltage. In all concentrations except 7 wt %, distribution of fiber's diameter (C.V.) increased with increasing D from 7 cm to 14 cm. Figure 2 presents the effect of concentration in each certain V and D on the average and distribution (C.V.) of fiber's diameter. As it is observed, in constant Vs and Ds, enhancement of concentration from 7 wt % to 8 wt % caused to increase the average fiber diameter, while from 9 wt % to 10 wt % decreased it. Also, it can be seen that, except for (13 kVp, 7 cm), in all constant Vs and Ds, the C.V. as a criterion of distribution of fiber's size decreased with increasing concentration.

The signal to noise (S/N) ratio is an appropriate value for indicating the real impact of each factor in obtained results and finding optimum conditions, which has the best response with the least variance. The S/N ratio of minimum average fiber diameter can be expressed as "smaller is better" and obtained from:

$$\mathrm{S/N} = -10 \log \text{ mean standard deviation (MSD)}$$

$$\mathrm{MSD} = (y_1^2 + y_2^2 + \ \ldots \ + y_n^2)/n$$

Where $n$ and $y$ are the numbers of observations and the experimental data, respectively.

The S/N ratio of the various levels of each factor affecting the average and distribution (C.V.) of the fiber's diameter is presented in Figure 3. In good agreement with authors' experiences and literature about the effectiveness of the selected factors, the S/N ratio plots show intensive effects of all the three factors on the intended results, since the S/N ratios have severe changes between various levels of each factor. As it is observed, in the case of S/N ratio plots related to the average fiber's diameter, the level 1 is the best level for every factor, which is 7 wt %, 9 kVp and 7 cm for concentration, V and D, respectively. On the other hand, according to the S/N ratio plots of each factor related to the C.V. of fiber's diameter, the best level of concentration is 3, which is 9 wt % and corresponding to maximum S/N ratio. Moreover, the best levels of V and D are 1 and 2, respectively. Since the uniformity of fibers (minimum distribution of fiber's diameter) is an essential feature than the fiber size, PHB 9 wt % solution (showed minimum C.V. and maximum S/N ratio) was electrospun by applying some other various Vs and Ds (Table II) to obtain the most uniform fibers.

Figure 4(A) shows the images of electrospun scaffolds obtained from PHB 9 wt % at various applied Vs and Ds. A large number of beads can be seen in specimens S4 and S6, which is attributed to the inappropriate conditions of electrospinning. Also, in other samples, except for sample S8, nonuniform bead-free fibers were obtained due to the inappropriate conditions. Most uniform bead-free fibers were obtained in D = 15 cm and V = 21 kVp, which has been identified as optimized specimens

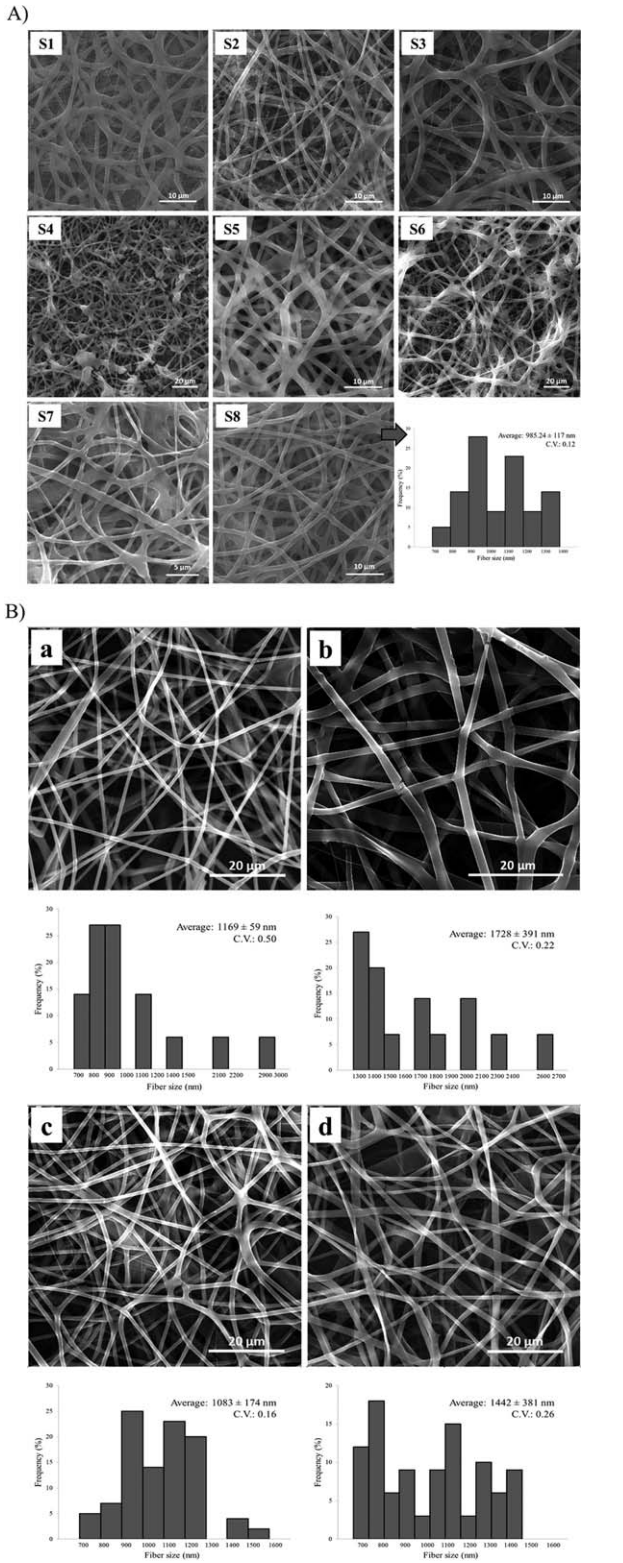


**Figure 4.** SEM images of: (A) PHB (9 wt %): S1) D = 11 cm V = 9 kVp, S2) D = 7 cm V = 13 kVp, S3) D = 15 cm V = 13 kVp, S4) D = 11 cm V = 17 kVp, S5) D = 15 cm V = 17 kVp, S6) D = 7 cm V = 21 kVp, S7) D = 11 cm V = 21 kVp, S8) D = 15 cm V = 21 kVp. (B) PHB (9 wt %)/CTS blend scaffolds (produced in D = 15 cm, V = 21 kVp): (a) 5% CTS, (b) 10% CTS, (c) 15% CTS, (d) 20% CTS.

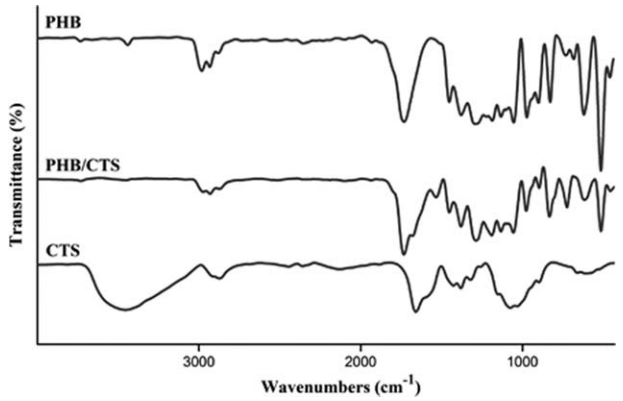


**Figure 5.** FTIR spectra of PHB, CTS and PHB/CTS blend.

for blending with CTS and further optimization. Distribution of fiber's diameter of this scaffold is shown in Figure 4(A). SEM images of scaffolds containing 5%, 10%, 15%, and 20% of CTS were shown in Figure 4(B). All the blend scaffolds had uniform fibers without any bead. As it is observed, specimens containing 5% of CTS had less uniform fibers compared to others. Contrary to the reported effects of CTS on poly(caprolactone)/CTS blend fibrous scaffolds, addition of CTS increased the fiber size and distribution of the fibrous scaffolds in this study.[38]

### FTIR

Figure 5 shows the FTIR spectra for electrospun PHB, CTS, and PHB/CTS blend. The FTIR spectrum of PHB has a characteristic peak at about 1731 $cm^{-1}$ assigned to the stretching vibration of the C═O group. Moreover, the peaks observed at about 973, 1293, and 1731 $cm^{-1}$ are attributable to the crystalline phase of PHB and peak at 1186 $cm^{-1}$ arises from the amorphous phase. In addition, the peak observed at about 1378 $cm^{-1}$ is related to the symmetric wagging of the $CH_3$ group. CTS has a characteristic peak at about 3455 $cm^{-1}$, corresponding to the OH and N-H groups stretching, while a peak seen at about 1660 $cm^{-1}$ is related to amide I. Identification of PHB crystallization using FTIR spectrum has been initially established by Bloembergen *et al.*[39] The C═O peak at about 1731 $cm^{-1}$ for pure PHB shifted to higher wavenumbers in PHB/CTS blend scaffolds proportional to the percentages of CTS. Increasing the wavenumber of the C═O group is a result of disturbances in the crystalline phase of PHB after addition of CTS.[40] This result is in agreement with the literature.[41] Also, peaks at about 973 $cm^{-1}$ and 1293 $cm^{-1}$ also shifted to higher wavenumbers. Presence and weakening of these peaks as a result of the addition of CTS are attributed to a decrease in crystallinity of PHB. Ikejima *et al.* reported that the C═O absorption peak related to the crystalline phase of PHB disappeared gradually with increasing amount of CTS in PHB/CTS blend and the peak corresponding to the amorphous phase increased.[42] The FTIR spectra indicated that CTS interacted with PHB via hydrogen bonds in the macromolecular region. In addition, the crystalline-related peaks of PHB weakened in the PHB/CTS blend fibers; the crystallinity of PHB was suppressed by CTS in the blend fibers via the chemical interaction between them (hydrogen bonds). This chemical interaction acts as a bridge between two polymers and accordingly, decreases the crystallinity, aiding the miscibility of the two polymers together.

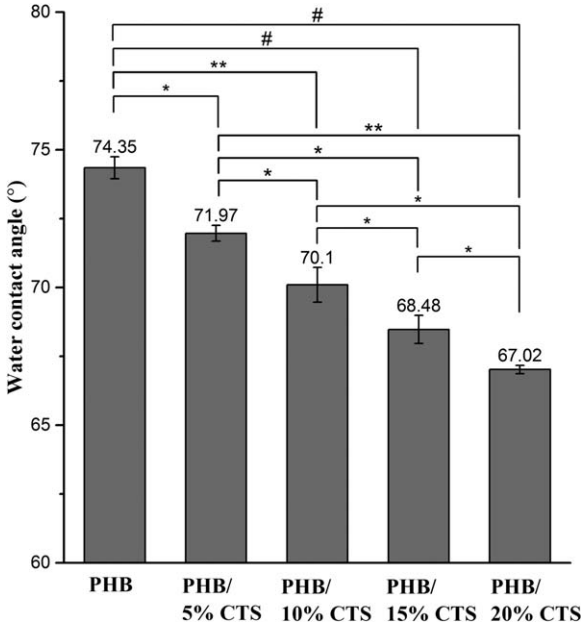


**Figure 6.** Contact angles of water droplets on the surfaces of PHB and PHB/CTS blend films (*$P < 0.05$, **$P < 0.003$, #$P < 0.0002$).

### WCA

Owing to the presence of hydrophilic functional groups on the polymer backbone of CTS,[43,44] it can increase the hydrophilicity of PHB through blending. The results showed that the addition of CTS to PHB increased the hydrophilicity of PHB and decreased its WCA from ~74° to ~67° ($P < 0.05$) which is related to PHB/20% CTS (Figure 6). Also, the addition of every concentration of CTS to PHB resulted in significant decreases in WCA of PHB ($P < 0.05$). Razavi *et al.* as well as Vaezifar *et al.* also reported the similar effect of CTS on decreasing the WCA of PLGA.[45,46]

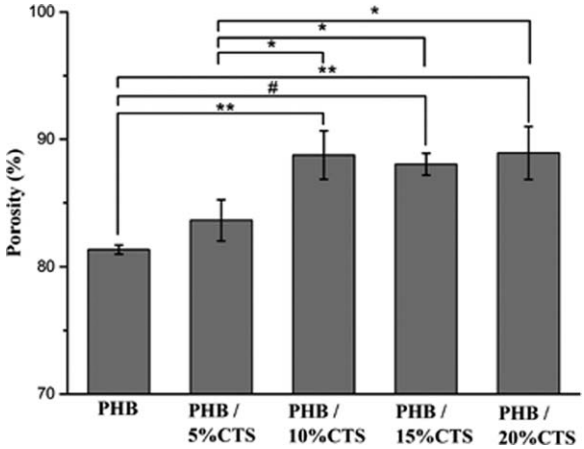


**Figure 7.** Porosity of PHB and PHB/CTS blend scaffolds (*$P < 0.05$, **$P < 0.003$, #$P < 0.0002$).

**Table III.** Mechanical Properties of Pure PHB and PHB/CTS Blend Scaffolds

| Sample | Tensile strength (MPa) | Young's modulus (MPa) | Toughness (MJ $m^{-3}$) | Elongation at break (%) |
|---|---|---|---|---|
| PHB | 87 ± 3.02 | 74.45 ± 2.88 | 1634.01 ± 6.9 | 26 ± 1.67 |
| PHB/5% CTS | 71.37 ± 2.82 | 51.34 ± 2.76 | 1875.15 ± 5.54 | 41.66 ± 1.46 |
| PHB/10% CTS | 63.66 ± 6.10 | 52.79 ± 4.52 | 1983.45 ± 7.83 | 46 ± 4.02 |
| PHB/15% CTS | 49.06 ± 3.12 | 57.80 ± 4.02 | 2460.01 ± 6.10 | 60 ± 3.97 |
| PHB/20% CTS | 31.6 ± 3.37 | 50.74 ± 2.23 | 2468.43 ± 5.86 | 65.5 ± 2.25 |

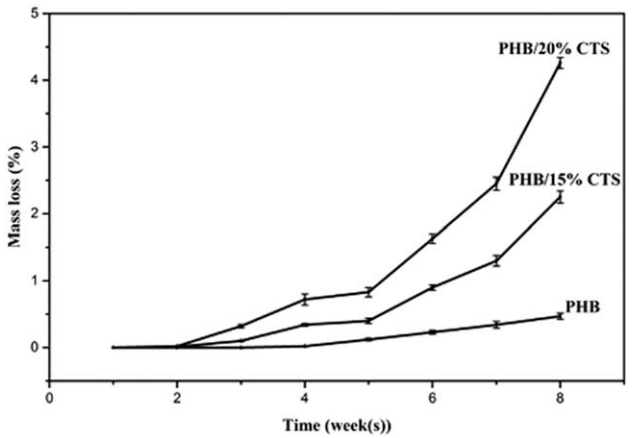


**Figure 8.** Mass loss percentages of the PHB and PHB/CTS blend fibrous scaffolds during 8 weeks.

### Porosity

Figure 7 presents porosity of the scaffolds. As it is observed, the addition of 10%, 15%, and 20% CTS to PHB resulted in significant increases in the porosity of the pure PHB scaffold. Also, there were significant differences between porosity of the PHB/5%CTS blend scaffold and that of the other blend scaffolds containing 10%, 15%, and 20%.

In fact, the relatively lowest porosity of PHB/5%CTS scaffold is due to the least uniformity of fiber's size in this scaffold compared to the other blend scaffolds (Figure 4). The other blend scaffolds containing 10%, 15%, and 20% of CTS showed more uniform fiber's sizes and thus higher porosities. The porosity of the blend scaffold containing 20% CTS was slightly more than other samples (88.92%). However, there was no significant difference between this sample with those containing 10% and 15% CTS. Contrary to these results, it has been reported that the porosity of PHB/gelatin blend electrospun scaffolds was decreased by enhancing the concentration of the gelatin (GEL).[47]

### Mechanical Properties

Mechanical properties of the scaffold are important in providing temporary support for cells.[48] Mechanical properties of the scaffolds containing 5%, 10%, 15%, and 20% CTS are shown in Table III. There was a direct relation between the percentage of CTS and the trend of tensile strength, Young's modulus, maximum strain and toughness of the scaffolds. By increasing the CTS, the tensile strength of the scaffolds gradually decreased from 87 MPa to ~31 MPa, which are related to pure PHB and PHB/20%CTS, respectively. In contrast, it has been reported that the tensile strength of PHB/GEL blend electrospun scaffolds decreased along with the increment of GEL content.[47] All the PHB/CTS blend scaffolds exhibited lower Young's modulus (in a range of about 50–57 MPa) compared to the PHB scaffold (~74 MPa). An increase in the CTS percentage in blend scaffolds from 5% to 15% increased Young's modulus from ~51 MPa to ~57 MPa, but, there is no significant difference between Young's moduli of the PHB/CTS blend scaffolds ($P > 0.05$). These changes in tensile strength and tensile modulus are related to the lower mechanical properties of CTS in comparison to the PHB. However, CTS can improve mechanical properties of the weaker polymers. Vaezifar *et al.* showed the improvement of mechanical properties of PLGA by the addition of CTS.[46] In another study, CTS could enhance the mechanical properties when it was used as a filler in poly(lactic acid)/CTS/epoxidized natural rubber composite.[49] The toughness of the scaffolds

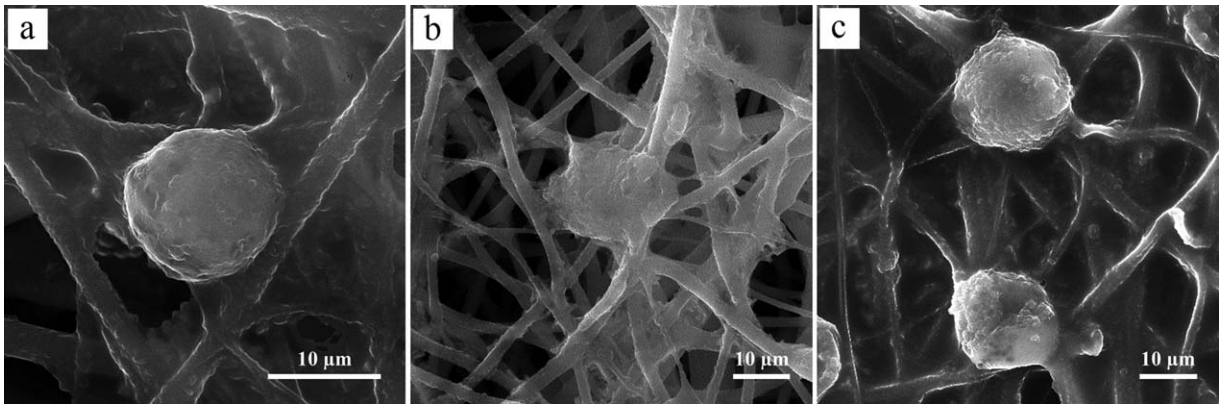


**Figure 9.** SEM images of cultured chondrocyte cells on the surface of (a) PHB, (b) PHB/15% CTS and (c) PHB/20% CTS scaffolds.

enhanced with increasing CTS in blend scaffolds from ~1634 MJ $m^{-3}$ to ~2468 M $Jm^{-3}$, which are related to pure PHB and PHB/20% CTS scaffolds, respectively. This increase is due to the tough nature of the CTS in comparison to PHB. Similarly, the maximum strain of the scaffolds increased from 26% to 65% by increasing CTS from 0% to 20%.

According to the SEM images and results of porosimetry, WCA, and tensile strength tests, PHB/CTS blend scaffolds containing 15% and 20% of CTS were identified as optimized scaffolds for *in vitro* mass loss and cell attachment studies.

### Mass Loss

Mass loss percentages of PHB, PHB/15% CTS, and PHB/20% CTS can be observed in Figure 8, indicating that the mass loss rate (and percentage) of the scaffolds increased by increasing the percentage of CTS, which is due to the higher mass loss rate of CTS compared to PHB. Vaezifar *et al.* and Shalumon *et al.* also reported a similar effect of CTS on the mass loss rate of PLGA and poly(lactic acid), respectively.[46,50]

### Cell Attachment

SEM images showed that chondrocytes attached well to the surfaces of all the samples (Figure 9). In pure PHB scaffold, the cells attached to the fibers did not spread well. However, in CTS comprising scaffolds, the chondrocytes attached, spread and slightly penetrated into the polymer matrix of the fibers, demonstrating that PHB/CTS blend scaffolds were more appropriate than the pure PHB scaffold. Razavi *et al.* also reported that CTS enhanced cell adhesion and proliferation on PLGA/CTS blend scaffolds.[45,51] In a similar study on PHB/CTS blend scaffolds fabricated by co-precipitation method, it was shown that CTS could increase the initial attachment of fibroblast cells.[41]

## CONCLUSIONS

In this study, PHB was successfully blended with CTS using TFA as a co-solvent and the blend solution was electrospun to fabricate fibrous scaffolds for cartilage tissue engineering. This study showed that the addition of CTS can increase hydrophilicity and mass loss rate (and percentage) of the electrospun PHB scaffolds while maintaining the mechanical properties in a suitable range for the intended application. In conclusion, the findings suggested a tremendous potential of the PHB/CTS blend fibrous scaffolds for further supplementary *in vitro* and *in vivo* studies in order to determine the suitability of these scaffolds for cartilage tissue engineering application.

## REFERENCES


1. Hunziker, E. *Osteoarthritis and Cartilage* **2002**, *10*, 432.
2. Karkhaneh, A.; Naghizadeh, Z.; Shokrgozar, M. A.; Bonakdar, S.; Solouk, A.; Haghighipour, N. *Int. J. Artif. Organs* **2014**, *37*, 142.
3. Johnstone, B.; Alini, M.; Cucchiarini, M.; Dodge, G. R.; Eglin, D.; Guilak, F.; Madry, H.; Mata, A.; Mauck, R. L.; Semino, C. E. *Eur. Cell Mater.* **2013**, *25*, 248.
4. Tuli, R.; Li, W. J.; Tuan, R. S. *Arthritis Res. Therapy* **2003**, *5*, 235.
5. Portocarrero, G.; Collins, G.; Livingston Arinzeh, T. *J. Tissue Sci. Eng.* **2013**, *4*, e120.
6. Johnstone, B.; Alini, M.; Cucchiarini, M.; Dodge, G. R.; Eglin, D.; Guilak, F.; Madry, H.; Mata, A.; Mauck, R. L.; Semino, C. E. *Eur. Cell Mater.* **2013**, *25*, e67.
7. Laurencin, C. T.; Nair, L. S. Nanotechnology and Regenerative Engineering: The Scaffold; CRC Press, **2014**, Section 1, p. 64.
8. Kumar, C. S. Biomimetic and Bioinspired Nanomaterials; Wiley, **2010**, Chapter 3, p. 91.
9. Teo, W. E.; He, W.; Ramakrishna, S. *Biotechnol. J.* **2006**, *1*, 918.
10. Huang, Z. M.; Zhang, Y. Z.; Kotaki, M.; Ramakrishna, S. *Compos. Sci. Technol.* **2003**, *63*, 2223.
11. Matsumoto, H.; Tanioka, A. *Membranes* **2011**, *1*, 249.
12. Sell, S. A.; Wolfe, P. S.; Garg, K.; McCool, J. M.; Rodriguez, I. A.; Bowlin, G. L. *Polymers* **2010**, *2*, 522.
13. Bhardwaj, N.; Kundu, S. C. *Biotechnol. Adv.* **2010**, *28*, 325.
14. Doyle, C.; Tanner, E.; Bonfield, W. *Biomaterials* **1991**, *12*, 841.
15. Luklinska, Z.; Schluckwerder, H. *J. Microscopy* **2003**, *211*, 121.
16. Masaeli, E.; Morshed, M.; Nasr-Esfahani, M. H.; Sadri, S.; Hilderink, J.; van Apeldoorn, A.; van Blitterswijk, C. A.; Moroni, L. *PloS One* **2013**, *8*, e57157.
17. Tehrani, A. H.; Zadhoush, A.; Karbasi, S.; Khorasani, S. N. *J. Appl. Polym. Sci.* **2010**, *118*, 2682.
18. Montazeri, M.; Karbasi, S.; Foroughi, M. R.; Monshi, A.; Ebrahimi-Kahrizsangi, R. *J. Mater. Sci.: Mater. Med.* **2015**, *26*, 1.
19. Ye, C.; Hu, P.; Ma, M. X.; Xiang, Y.; Liu, R. G.; Shang, X. W. *Biomaterials* **2009**, *30*, 4401.
20. Sombatmankhong, K.; Suwantong, O.; Waleetorncheepsawat, S.; Supaphol, P. *J. Polym. Sci. Part B: Polym. Phys.* **2006**, *44*, 2923.
21. Fryczkowski, R.; Kowalczyk, T. *Synthetic Metals* **2009**, *159*, 2266.
22. Hinüber, C.; Häussler, L.; Vogel, R.; Brünig, H.; Heinrich, G.; Werner, C. *Expr. Polym. Lett.* **2011**, *5*, 643.
23. de Alvarenga, E. S. *Biotechnol. Biopolym.* **2011**, *91*, 112.
24. Sechriest, V. F.; Miao, Y. J.; Niyibizi, C.; Westerhausen–Larson, A.; Matthew, H. W.; Evans, C. H.; Fu, F. H.; Suh, J. K. *J. Biomed. Mater. Res.* **2000**, *49*, 534.
25. Lahiji, A.; Sohrabi, A.; Hungerford, D. S.; Frondoza, C. G. *J. Biomed. Mater. Res.* **2000**, *51*, 586.
26. Suh, J. K. F.; Matthew, H. W. *Biomaterials* **2000**, *21*, 2589.
27. Senköü, A.; Simsek, A.; Sahin, F. I.; Menevse, S.; Özogul, C.; Denkbas, E. B.; Piskin, E. *J. Bioactive Compat. Polym.* **2001**, *16*, 136.
28. Cárdenas T, G.; Sanzana L, J.; Mei, I.; Lucia, H. *Boletín de la Sociedad Chilena de Química* **2002**, *47*, 529.

29. Davidson, M. J.; Balasubramanian, K.; Tagore, G. *J. Mater. Process. Technol.* **2008**, *200*, 283.
30. Hou, T. H.; Su, C. H.; Liu, W. L. *Powder Technol.* **2007**, *173*, 153.
31. Ashtiani, H. A. D.; Farsani, R. E. *Fibers Polym.* **2011**, *12*, 1054.
32. Saligheh, O.; Eslami-Farsani, R.; Khajavi, R.; Forouharshad, M. *Fibers Polym.* **2013**, *14*, 1864.
33. Chakrapani, V. Y.; Gnanamani, A.; Giridev, V.; Madhusoothanan, M.; Sekaran, G. *J. Appl. Polym. Sci.* **2012**, *125*, 3221.
34. Godoi, F.; Pereira, N.; Rocha, S. *Chem. Eng. Process.: Process Intensification* **2011**, *50*, 623.
35. Badwan, A.; Al-Remawi, M. Google Patents **2006**. Available at: http://www.google.com/patents/CA2616470A1?cl=en.
36. ASTM D882-12, Standard Test Method for Tensile Properties of Thin Plastic Sheeting, ASTM International, West Conshohocken, PA, 8 **2012**. Available at: http://www.astm.org/Standards/D882.
37. Pillay, V.; Dott, C.; Choonara, Y. E.; Tyagi, C.; Tomar, L.; Kumar, P.; du Toit, L. C.; Ndesendo, V. M. *J. Nanomater.* **2013**, 2013. Available at: http://www.hindawi.com/journals/jnm/2013/789289/abs/.
38. Van der Schueren, L.; Steyaert, I.; De Schoenmaker, B.; De Clerck, K. *Carbohydr. Polym.* **2012**, *88*, 1221.
39. Bloembergen, S.; Holden, D. A.; Hamer, G. K.; Bluhm, T. L.; Marchessault, R. H. *Macromolecules* **1986**, *19*, 2865.
40. Xu, J.; Guo, B. H.; Yang, R.; Wu, Q.; Chen, G. Q.; Zhang, Z. M. *Polymer* **2002**, *43*, 6893.
41. Medvecky, L.; Giretova, M.; Stulajterova, R. *J. Mater. Sci.: Mater. Med.* **2014**, *25*, 777.
42. Ikejima, T.; Yagi, K.; Inoue, Y. *Macromol. Chem. Phys.* **1999**, *200*, 413.
43. Kim, S.-K. Chitin and Chitosan Derivatives: Advances in Drug Discovery and Developments; CRC Press, **2013**, Chapter 2, pp. 16.
44. Stafsnes, M.; Bruheim, P. *Diversity, and Characterization of Pigmentation* **2013**, 117. Available at: https://www.crcpress.com/Marine-Biomaterials-Characterization-Isolation-and-Applications/Kim/p/book/9781466505643.
45. Razavi, S.; Karbasi, S.; Morshed, M.; Esfahani, H. Z.; Golozar, M.; Vaezifar, S. *Cell J. (Yakhteh)* **2015**, *17*, 429.
46. Vaezifar, S.; Razavi, S.; Golozar, M. A.; Esfahani, H. Z.; Morshed, M.; Karbasi, S. *Int. J. Polym. Mater. Polym. Biomater.* **2015**, *64*, 64.
47. Nagiah, N.; Madhavi, L.; Anitha, R.; Srinivasan, N. T.; Sivagnanam, U. T. *Polym. Bull.* **2013**, *70*, 2337.
48. Hollister, S. J. *Nat. Mater.* **2005**, *4*, 518.
49. Zakaria, Z.; Islam, M. S.; Hassan, A.; Mohamad Haafiz, M.; Arjmandi, R.; Inuwa, I.; Hasan, M. *Adv. Mater. Sci. Eng.* **2013**, 2013. Available at: http://www.hindawi.com/journals/amse/2013/629092/abs/.
50. Shalumon, K.; Sathish, D.; Nair, S.; Chennazhi, K.; Tamura, H.; Jayakumar, R. *J. Biomed. Nanotechnol.* **2012**, *8*, 405.
51. Razavi, S.; Zarkesh-Esfahani, H.; Morshed, M.; Vaezifar, S.; Karbasi, S.; Golozar, M. A. *J. Biomed. Mater. Res. Part A* **2015**, *103*, 2628.